Int. J. Radiat. Biol., Vol. 86, No. 12, December 2010, pp. 1106–1116

informa
healthcare

Pulse modulated 900 MHz radiation induces hypothyroidism and apoptosis in thyroid cells: A light, electron microscopy and immunohistochemical study

MERİÇ ARDA EŞMEKAYA[1], NESRIN SEYHAN[1], & SUNA ÖMEROĞLU[2]

[1]*Department of Biophysics, Faculty of Medicine & Gazi Non-ionizing Radiation Protection (GNRP) Center and*
[2]*Department of Histology and Embryology, Faculty of Medicine, Gazi University, Ankara, Turkey*

(Received 7 April 2010; Revised 15 June 2010; Accepted 17 June 2010)

Abstract

Purpose: In the present study we investigated the possible histopathological effects of pulse modulated Radiofrequency (RF) fields on the thyroid gland using light microscopy, electron microscopy and immunohistochemical methods.

Materials and methods: Two months old male Wistar rats were exposed to a 900 MHz pulse-modulated RF radiation at a specific absorption rate (SAR) of 1.35 Watt/kg for 20 min/day for three weeks. The RF signals were pulse modulated by rectangular pulses with a repetition frequency of 217 Hz and a duty cycle of 1:8 (pulse width 0.576 ms). To assess thyroid endocrine disruption and estimate the degree of the pathology of the gland, we analysed structural alterations in follicular and colloidal diameters and areas, colloid content of the follicles, and height of the follicular epithelium. Apoptosis was confirmed by Transmission Electron Microscopy and assessing the activites of an initiator (caspase-9) and an effector (caspase-3) caspases that are important markers of cells undergoing apoptosis.

Results: Morphological analyses revealed hypothyrophy of the gland in the 900 MHz RF exposure group. The results indicated that thyroid hormone secretion was inhibited by the RF radiation. In addition, we also observed formation of apoptotic bodies and increased caspase-3 and caspase-9 activities in thyroid cells of the rats that were exposed to modulated RF fields.

Conclusion: The overall findings indicated that whole body exposure to pulse-modulated RF radiation that is similar to that emitted by global system for mobile communications (GSM) mobile phones can cause pathological changes in the thyroid gland by altering the gland structure and enhancing caspase-dependent pathways of apoptosis.

Keywords: *radiofrequency radiation, thyroid gland, apoptosis, hypothyroidism, electromagnetic field*

Introduction

The usage of mobile phones has been substantially increasing and there is a considerable concern about possible health hazards of mobile phone radiation. Some studies actually showed a higher brain cancer risk in people who had used mobile phones for more than ten years (Hardell et al. 2008). The results of the INTERPHONE study suggested a possible relation between mobile phone use (at high exposure levels) and risk of glioma. The risk for glioma tended to be greater in the temporal lobe than in other lobes of the brain (The INTERPHONE Study Group 2010). For both analogue and digital mobile phones, the signals transmitted and received are in the form of waves in the radiofrequency (RF) part of the Electromagnetic Spectrum which is modulated by low frequency information signals. Since the quantum photon energy of the RF radiation (RFR) is not sufficient to cause ionisation of atoms, its biological effects on tissues may be explained by thermal and non-thermal mechanisms. Non-thermal effects of the RF radiation occur at the levels of the energy which is unlikely to increase the temperature of the tissue, nevertheless physical or biochemical changes are induced at these energy levels. In recent years, there have been many epidemiological and animal studies reporting a variety of biological effects caused by RFR. Molecular and cellular effects of RFR exposure have been reported, including strand-break in DNA, gene expressions, release of calcium from intracellular storage sites (Lai and Singh 1996,

Correspondence: Dr Meriç Arda Eşmekaya, Department of Biophysics, Gazi University, Faculty of Medicine, Gazi University, 06510 Beşevler, Ankara, Turkey. Fax: +90 31221 29023. E-mail: mericarda@yahoo.com

ISSN 0955-3002 print/ISSN 1362-3095 online © 2010 Informa UK, Ltd.
DOI: 10.3109/09553002.2010.502960

Pacini et al. 2002, Buttiglione et al. 2007) cell proliferation inhibition (French et al. 1997), and alteration of membrane channels (Apollonio et al. 1997). Although the mechanism by which RFR exerts these effects remained unclear, some authors pointed out a possible role of free radical formation inside cells (Garaj et al. 2009). It is known that free radicals kill cells by damaging macromolecules, such as DNA and proteins. Several studies have showed that electromagnetic fields enhance free radical activity in biological cells and tissues (Zmyślony et al. 2004, Luukkonen et al. 2009).

Apoptosis is a highly regulated and evolutionary conserved pathway of cell death that plays a critical role in development and maintenance of tissue homeostasis. Disturbances in apoptosis regulation could lead to many diseases (Hashimoto 1996). It is involved in the homeostasis of follicular cells of the thyroid gland as well as in the destructive mechanisms of autoimmune thyroiditis such as Hashimoto's Thyroiditis (HT) and cell death in thyroid cancer. The caspases (Cysteinyl-aspartate-specific proteinases), that are the family of the cysteine proteases and the members of the interleukin-1β-converting enzyme family, are one of the main executors of the apoptotic process. They have an importance role in the apoptotic signaling network which are activated in most cases of apoptotic cell death. Caspase-9 plays a central role in cell death induced by a wide variety of apoptosis inducers including tumour necrosis factor-alpha (TNFa), tumour necrosis factor-related apoptosis-inducing ligand (TRAIL), fatty acid synthase/apolipoprotein-1 (Fas/Apo1), fas-associated protein with death domain (FADD), and tumour necrosis factor receptor-associated death domain protein (TRADD). Caspase-9 cleaves and activates the apical effector caspases such as caspase-3 that is one of the key executioner of apoptosis, being responsible either partly or totally for the proteolytic cleavage of many key proteins, and the activated form of it is a marker of cells undergoing apoptosis (Gerald 1997, Lin 2001). Some of the in vitro studies have reported induction of caspase-dependent and caspase-independent apoptotic pathways attributable to RFR exposure. Menadione-induced caspase-3 activity was increased in mouse L929 fibroblast cells as a result of exposure to a 872 MHz modulated RFR at a specific absorption rate (SAR) of 5 W/kg in isothermal conditions for 1 or 24 h (Höytö et al. 2008). Time-dependent apoptosis (45% for 3 h) was reported by Caraglia et al. (2005) in human epidermoid KB cancer cells derived from squamous head and neck cancer after exposure to a 1.95 GHz continuous-wave RFR at 3.6 W/kg for 1–3 h. Joubert et al. (2008) has observed increased caspase-3 independent apoptosis in rat primary neuronal cultures exposed to a 900 MHz continuous-wave RFR at 2 W/kg for 24 h. Increased percentage of early apoptotic retinal ganglion cells were reported by Zhou et al. (2008) after exposure to a 2,450-MHz RFR at 30 mw/cm^2 and 60 mW/cm^2 for 1 h. However, negative results have been also reported depending on cell type and exposure characteristics (Hook et al. 2004, Joubert et al. 2007).

The thyroid gland plays an essential role in regulation of body growth, development, metabolism and activity of nervous system and disturbances of the thyroid gland have striking effects in metabolism of the body as a whole. Studies have shown that RFR has effects on the thyroid gland (Black and Heynick 2003) including morphological and functional alterations of the gland. A decrease in serum thyroid-stimulating hormone (TSH) level has been reported in male volunteers who were exposed to global system for mobile communications (GSM) modulated RF radiation for 2 h/day for a month (De Seze et al. 1998). Similarly, lower levels of TSH and thyroid hormones (TH) were revealed in animal studies as a result of exposure to continuous-wave RFR (Koyu et al. 2005).

In this study, we investigated the possible histopathological effects of a 900 MHz pulse-modulated RFR on the thyroid gland using light microscopy, electron microscopy and immunohistochemical methods. Thyroid cells undergoing apoptosis were identified by electron microscopy and activities of an initiator (caspase-9) and an effector (caspase-3) caspases which are important markers of cells undergoing apoptosis.

Materıals and methods

Experimental animals and treatments

The study was conducted on two-month old male Wistar rats (weighing 200–300 g) purchased from the Hıfsızsıhha Institute. Animals were housed in a room maintained at $22 \pm 1^{\circ}$C and $50 \pm 10\%$ humidity, and under 12-h light-dark cycle (light in room 07:00– 19:00 h). Rats were fed commercial rat chow and given water *ad libitum*. None of the animals died during the experiment. The investigation was carried out in accordance with national and international laws and approved by the Local Ethics Committee of Gazi University Faculty of Medicine. At the beginning of the experiment, the animals were divided randomly into three groups: cage-control group ($n = 10$), sham-exposed group ($n = 10$), and 900-MHz pulse-modulated RF radiation exposed group ($n = 10$). The RF-group was exposed to a 900-MHz pulse-modulated RF radiation 20 min/day for 21 days. The sham-exposed group rats were subjected to the same experimental procedure of the RF-exposed group except that the signal generator

was turned off. Rats of the cage-control group were housed in their home cages during the entire experimental period without subjecting to any experimental manipulation. The rats were sacrificed by decapitation following anesthesia by intramuscular injection of ketamine (50 mg/kg) and xylazine (5 mg/kg).

Exposure system

The exposure system consisted of a RF generator (Agilent Technologies, Santa Clara, CA, USA) that produced the 900 MHz RF signals, a power amplifier (Hittite, Chelmsford, MA, USA) that amplified the output power of the RF generator, an arbitrary function generator (Thandar, Cambridgeshire, UK) that applied the pulse modulation input of the RF generator, and a rectangular (20–25 cm) horn antenna (ETS-Lındgren, St Louis, MO, USA) facing upwards (Figure 1). The RF signals were pulse modulated by rectangular pulses with a repetition frequency of 217 Hz and a duty cycle of 1:8 (pulse width 0.576 ms). 217-Hz pulse signals were observed and verified by using an oscilloscope. Polymethyl methacrylate plastics cage (15 × 20 × 20 cm) which the rats were housed in was placed symmetrically along the axis which is perpendicular and 10 cm above the mid-line of the horn antenna. The cage was constantly aerated to avoid the possibility of any increase in temperature inside the cage. To obtain sufficient field intensity, a cage was placed in the near field of the antenna. Electric field measurements were performed along the horn antennas axis by using an isotropic probe (Rohde and Schwarz, Munich, Germany) and a handheld spectrum analyser RandS®FSH4 (Rohde and Schwarz, Munich, Germany). The RF environmental background level in the frequency range of 30 MHz to 3 GHz was 0.1–0.22 V/m.

At the beginning of exposure, average power density was measured at a reference point which was the mid-point of the bottom of the cage wall facing the horn antenna. The maximum power density was observed along the axis of the antenna and it decreased uniformly with the distance from the antenna's axis.

SAR is a measure of the rate of radiation energy absorption per unit weight of tissue and is expressed in units of watts per kilogram (W/kg). It is a widely used dosimetric quantity to compare the absorbed energy in different biological tissues. The SAR value was estimated by measurements and calculations in this experiment.

SAR was computed using the following equation:

$$\mathrm{SAR} = \sigma/\rho\,|\mathrm{E_{RMS^2}}|[\mathrm{W/kg}]$$

where; E_{RMS} is the root mean square value of the electric field (V/m), σ is the mean electrical conductivity of the tissues in siemens/meter (S/m) and ρ is the mass density (kg/m^3) (International Commission on Non-Ionizing Radiation Protection [ICNIRP] 1998, Institute of Electrical and Electronics Engineers/American National Standards Institute [IEEE/ANSI] IEEE C95.1–1991). The rat body was assumed an equivalent tissue based on the average of the dielectric properties of the 36 tissues in the rat segmented at Brook Air Force Base. Conductivity (0.87 S/m) and mass density (1105 kg/m^3) were derived for the equivalent tissue by using dielectric properties and mass densities of these tissues. The RF exposure in the experiment resulted in a whole body average SAR of 1.35 W/kg with an E_{RMS} field of 41 V/m.

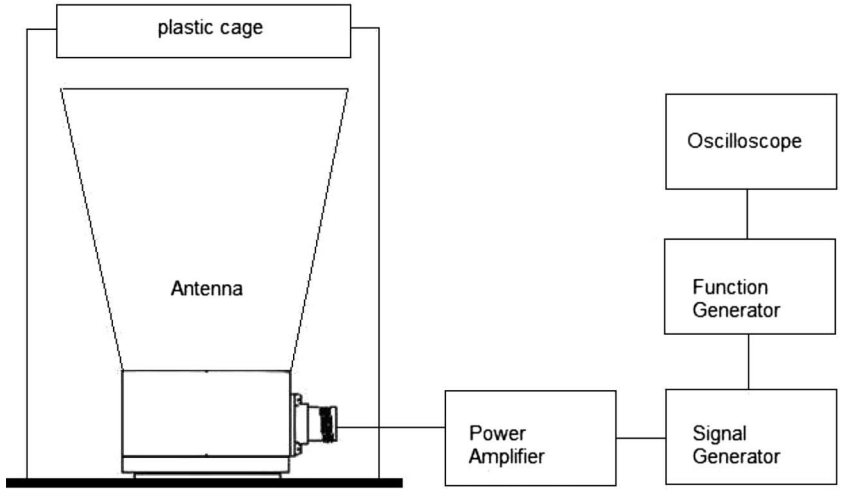

Figure 1. Schematic diagram of the RF exposure system.

Body temperature of rats was recorded by rectal measurements prior and after exposure session. The RF exposure resulted in a mean rectal temperature increase of 0.2°C.

Histological assesment

After sacrification, thyroid glands of the rats were immediately excised, trachea and adherent tissue attached to the thyroid gland was removed. Specimens were taken from the middle of the right lobes and fixed in 10% neutral phosphate-buffer formaldehyde solution for 24 h at room temperature. After fixation, the specimens were dehydrated in a graded alcohol series, embedded in paraffin wax, and cut into 5 μm sections, deparaffinised in xylene and stained in Hematoxylin and Eosin (Merck, Darmstadt, Germany).

Immunohistochemistry

Formalin-fixed paraffin embedded tissue blocks were cut at 5 μm and mounted on poly-L-lysine coated glass line, then deparaffinised and dehydrated with xylene and graded alcohol. Slides were washed in PBS (Phosphate Buffered Saline) and treated in a microwave oven in 10% citrate buffer at pH 6 for antigen retrieval. After incubation of the slides for 20 min in room temperature, they were enrolled with a pap-pen (hydrophobic pen). Endogenous peroxidase activity was blocked by immersing the slides in 3% hydrogen peroxide. Application of ultra V block was followed by incubation of the slides with the primary antibodies to caspase-3 and caspase-9 (Lavvision/NeoMarkers Corporation, USA) cleaved for 30 min at room temperature. Finally the slides were counterstained with hematoxylin then dehydrated and mounted. All the slides were evaluated with a DM 2000B light microscope (Leica, Germany).

Electron microscopy

For the transmission electron microscope (TEM) analyses, thyroid glands were excised and prefixed immediately in 2.5% glutaraldehyde solution in 0.1 M sodium cacodylate buffer (pH 7.4) for 2 h at room temperature. The tissues were then fixed in a similarly buffered solution of 1% osmium tetraoxide (Sigma, St Louis, MO, USA) for 2 h at 4°C. Specimens were dehydrated through a graded series of acetone and then in propylene oxide and embedded in Araldite (Sigma, USA) and dodecenylsuccinicanhydride (DDSA). One micrometer semi-thin cut sections were stained by toluidine blue to select the region of interest. Ultra-thin sections obtained with an ultramicrotome using a diamond knife were collected on 150 mesh copper grids and stained with uranyl acetate and lead citrate. The sections were examined and photographed using a LEO 906 E TEM (Carl Zeiss, Oberkochen, Germany).

Histomorphometrical examination of the thyroid gland

Morphological appearance of the thyroid follicles, follicular epithelium cells, and the content of the colloid show variations according to the functional activity of the thyroid gland. To show thyroid endocrine disruption, several parameters were accurately measured to characterise the structural changes in the gland. To estimate the degree of pathology and the activity of the thyroid gland, alterations in the diameter and area of the follicles, diameter and area of the colloids, the content of the colloid in the follicles, and height of follicular epithelial cells of the thyroid gland were analysed. Photomicrographs of the each thyroid follicle in randomly selected areas were obtained by a Leica light microscope. The follicular and colloidal area and diameter of 50 randomly selected follicles and colloids were measured in each of 10 randomly chosen fields using a Qwin3 software (Leica, Germany). Thus, 500 follicular and colloidal area and diameter from each animal was measured. The area of the colloid was measured by calculating the area enclosed by the apical surface of the follicular epithelium cells. The colloid content of the follicles in the vesicle was obtained by using an ocular containing a grid and 40× magnification. The height of 10 randomly selected epithelial cells was measured in 10 randomly chosen fields at 400× magnification with an ocular micrometer. The average values for each parameter was calculated for each gland and the averages were treated as individual values. All data were presented as mean values ± standard deviation (SD). Differences among the three treatment groups were analysed by the one-way analysis of variance (ANOVA). The Tukey's Honestly Significant Difference (HSD) test was used for pairwise comparisons between groups. The accepted level of significance was set at $p < 0.05$.

Evaluation of the immunohistochemical staining

Immunohistochemical findings were scored by using the Immunoreactive Scoring System (IRS) depending on the extent and intensity of positively staining thyroid follicular cells in 10 randomly selected fields. The intensity of staining was graded semi-quantitatively on a four points scale: 0 (negative), 1 (weak), 2 (moderate), and 3 (strong). The extent of positive immunoreactivity was scored according to the percentage of positively stained thyroid follicular

cells for the active caspase-9 and caspase-3 as follow: 0 (0%), 1 (1–25%), 2 (26–50%), 3 (51–75%), and 4 (76–100%). An overall final score was obtained in each case by adding the intensity to the extent score. Tissues having a final staining score of two or more were considered to show positive expression. A final staining score of 2–3 was considered weak expression (+), 4–5 was moderate expression (++), and 6–7 was strong expression (+++). All slides were graded independently by two pathologists without previous knowledge of exposure history of the samples. The final scores of staining were given as mean ± standard deviation (SD). Data were analysed by the Kruskal-Wallis and Dunnett's multiple comparison post hoc tests. Differences were considered to be significant at $p < 0.05$.

Results

Thyroid morphometry

Figure 1 illustrates characteristic microscopic pictures of the thyroid follicles of cage-control, sham- and RF-exposed rats. Thyroid glands of the rats exposed to pulse-modulated RF radiation showed a high prevalence of cell hypothyrophy. Oval and round shaped macro-follicles with denser colloid were dominant in the thyroid glands of RF-exposed rats. Because of the fact that the whole gland appeared to have a macro-follicular structure, the lumina became smaller in RF-exposed thyroids. Small to medium follicles were predominant in thyroids of sham-exposed and cage-control rats. However, some large follicles were seen in each group. Follicular architecture of the cage-control and sham groups showed a considerable heterogeneity. Small amount of colloid droplets was seen in cage-control thyroids suggesting an active gland with microvilluses in the apical surface. Follicular structure was destroyed (Figure 4c, 4d) and follicular cells were irregular in shape and distribution in the RF-exposed group.

In contrast to cage-control and sham thyroids, electron dense lysosomes in apical cytoplasm were seen in the RF-exposed thyroids. Low prismatic round shape nuclei were settled in the cage-control group (Figure 2a). The nucleus of the RF-exposed thyroids were observed in the basal line. The shape of the RER (rough endoplasmic reticulum) and the nuclei were regular in sham thyroids (Figure 3b). A remarkable crista lost in the mitochondria and apoptotic bodies were noticeable in thyroid cells of RF-exposed group (Figure 3c, 3d).

RF-exposed rats had higher follicle diameters in their thyroid glands compared to sham and cage-control rats ($p < 0.001$). Similarly, diameters of colloids increased significantly in the RF-exposed group ($p < 0.001$). However, follicular and colloidal diameters did not show any significant difference between the sham and cage-control groups

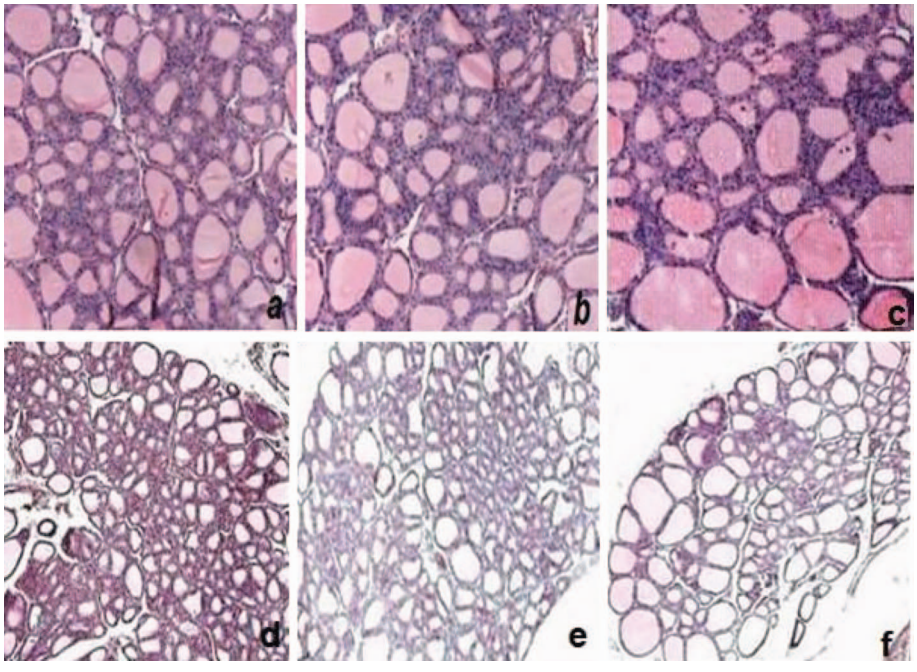

Figure 2. Photomicrographs of the thyroid sections from representative control (a), sham (b) and RF-exposed (c) rats. RF exposed group thyroids presented comparatively large thyroid follicles filled by a variable quantity of dense colloids, Hematoxylin and Eosin Magnification × 40. Note that macrofollicles are dominant in exposed thyroids (f). Control (d) and sham (e) thyroids were characterised by small to medium follicles with less dense colloid, Hematoxylin and Eosin magnification × 10.

($p > 0.05$) (Figure 5b). Follicular area increased significantly in RF-exposed thyroids than those of cage-control and sham thyroids ($p < 0.001$). As seen in Figure 2c, some follicles were greatly increased in size in the RF-exposed group. Follicular area did not differ significantly in sham and cage-control thyroids ($p > 0.05$) (Figure 4a). The change in follicular area in RF-exposed group was accompanied with a significant increase in the colloidal area. The overall colloid area increased significantly in the RF-exposed group in comparison with the sham and cage-control groups ($p < 0.001$). Colloid area did not differ signifantly between the sham and cage-control groups ($p > 0.05$) (Figure 5a). The proportion of the colloid matter in the thyroids of the RF-exposed rats increased significantly compared to the corresponding cage-control and sham colloid contents ($p < 0.001$). Colloid matter occupied 89% of the total thyroid area in the RF-exposed group, whereas sham and cage-control rats had less colloid present in their thyroid glands (Figure 5e). A significant decrease was seen in the follicular cell height of the thyroids in the RF-exposed group than the sham and cage-control groups ($p < 0.001$). However, the height of the follicle epithelium cells in the RF-exposed group was sigificantly reduced ($P < 0.001$) by 23% and 27%, respectively, when compared with those of the sham and cage-control groups (Figure 5c).

Immunohistochemical results

A semi-quantitative analysis of the RF-exposed thyroids showed moderate to high caspase-9 cleaved immunoreactivity in follicular cells, apical membrane, interstitial connective tissue, and colloids in the follicular lumen. The staining of caspase-9 antibody was also remarkable *in* parafollicular cells in the RF-exposed group (Figure 6e). The overall final immunoreactive score which was obtained from the sum of intensity and extent scores was 6.3 in the RF-exposed group showing a strong expression (+++) (Table I). It was significantly higher ($p < 0.01$) than the final immunoreactive scores of the sham (2.1) and cage-control (2.5) groups (Table I). The specimens of sham (Figure 6d) and

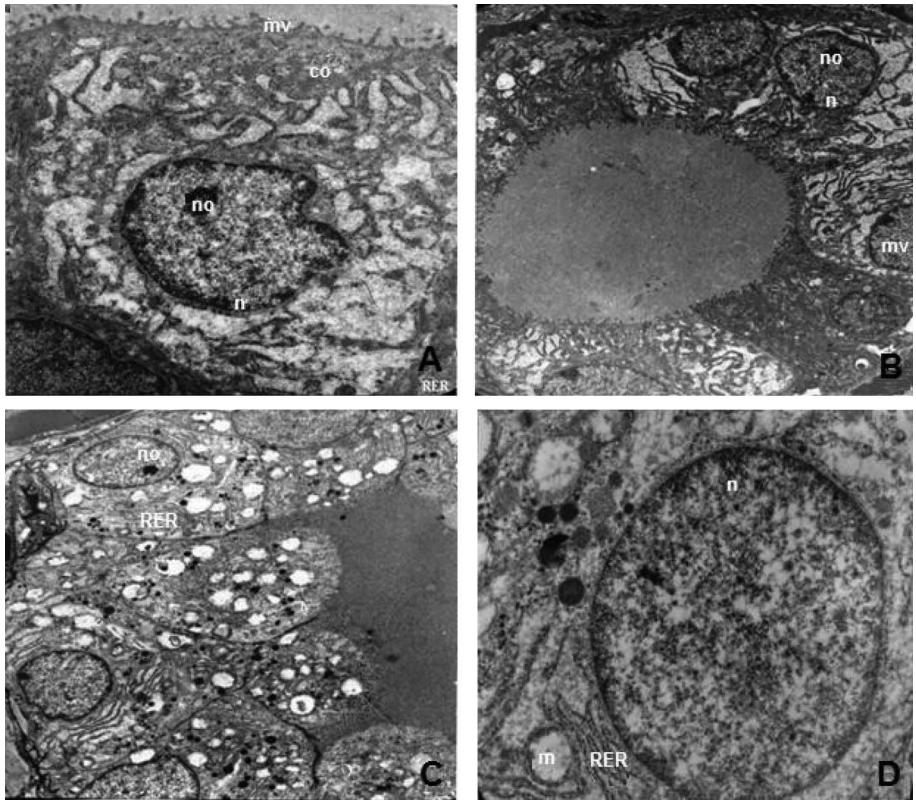

Figure 3. (a) Control group: nucleus (n), nucleolus (no), rough endoplasmic reticulum (RER) and microvilli (mv) are seen in the cell forming the follicular wall of the thyroid gland (Lead citrate-uranyl acetate × 2784); (b) Sham group: In the follicular unit forming the thyroid gland follicular cells within the wall; n, no, RER and mv are located on the apical surface facing towards the follicular lumen (mu) (Lead citrate-uranyl acetate × 2784); (c) RF-exposed group: In the follicular unit belonging to the thyroid gland, several follicular cells forming the follicular wall and having n, no, many pleomorfic lysosom (ly) and mitochondria losing crista are seen. Apopotic changes are seen on the upper left corner of the figure. (Lead citrate-uranyl acetate × 2784); (d) In the greater magnification of the RF-exposed group follicular cell, nucleus (n), RER and mitochondria showing cristalysis can be seen in detail. (Lead citrate-uranyl acetate × 10,000)

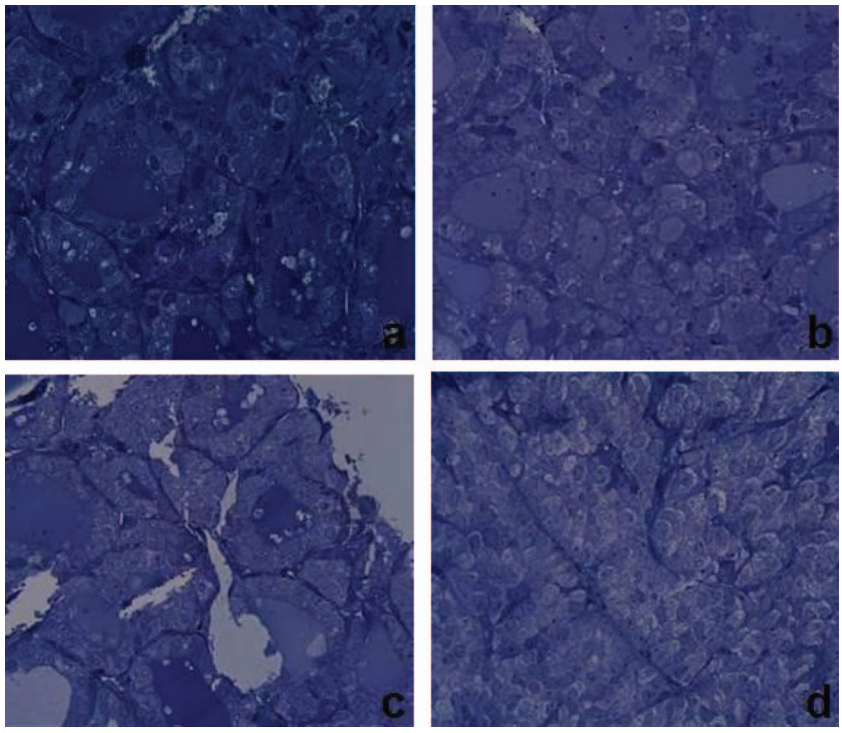

Figure 4. Toluidine Blue staining of control (a), sham (b) and RF-exposed group (c, d) thyroid specimens. Note the destruction of follicular architecture in RF-exposed group, Magnification × 40.

Table I. Final immunoreactive scoring of Caspase-9 ans Caspase-3 expressions.

Caspase-9	Mean ± SD	Caspase-3	Mean ± SD
Control ($n = 10$)	2.39 ± 0.16	Control ($n = 10$)	1.54 ± 0.2
Sham ($n = 10$)	1.99 ± 0.49	Sham ($n = 10$)	1.39 ± 0.13
Exposed ($n = 10$)	4.63 ± 0.34*	Exposed ($n = 10$)	4.32 ± 0.29*

The data represent mean ± SD of 10 independent experiments. *Significantly different between exposed and control or sham groups ($p < 0.01$) by Kruskal-Wallis and Dunnett's Multiple Comparison Post Hoc tests.

cage-control groups (Figure 6c) showed a weak (+) caspase-9 immunolabeling and no significant difference were observed between these groups ($p > 0.05$). We found a positive caspase-3 immunoreactivity with a predominance of strong expression (+++) in follicular cells, apical membrane, interstitial connective tissue and parafollicular cells in the RF-exposed group (Figure 6b). The sham (Figure 6a) and cage-control groups showed a weak positive (+) caspase-3 immunoreactivity in follicular cells. The final immunoreactive score in the RF-exposed group was 6.1 (Table I), which was significantly higher ($p < 0.01$) than those of the sham and cage-control groups. There was no statistically difference between sham (2.4) and cage-control (2.7) groups (Table I) ($p > 0.05$) in terms of final immunoreactivity scores.

Dıscussıon and conclusion

Histopathological examination of the thyroid gland of the cage-control, sham- and RF-exposed rats showed significant pathlogical changes in the thyroid glands of the RF-exposed rat. Exposure to pulse-modulated RF radiation caused striking changes in the thyroid structure. Morphometrical analysis revealed hypothyrophy of the gland in the RF-exposed group. A significant decrease in follicular epithelium height suggested unstimulated and resting follicular cells in the RF-exposed group. It is known that follicle epithelium height depends on the functional state of the thyroid gland and lower follicular epithelium height is related with resting follicular cells (Ingbar 1985). The diameter and area of the colloid in the lumen of the follicles of the RF-exposed group increased significantly. This indicates that thyroid glands of the RF-exposed rats were in an inactive state. Resting follicles are usually associated with increased thyroid colloidal area. Inhibition of phagocytosis/pinocytosis of the colloid that contains thyroglobulin causes it to accumulate in the follicular lumen, thereby increasing the colloidal diameter and diminishing the height of the follicular epithelium. An inhibition of the pinocytosis and endocytosis processing of thyroglobulin from the colloid causing a decrease in thyroid secretion and increase in collloid content has been reported (Denef et al. 1989, Castillo et al. 2003, Wollman et al. (1990).

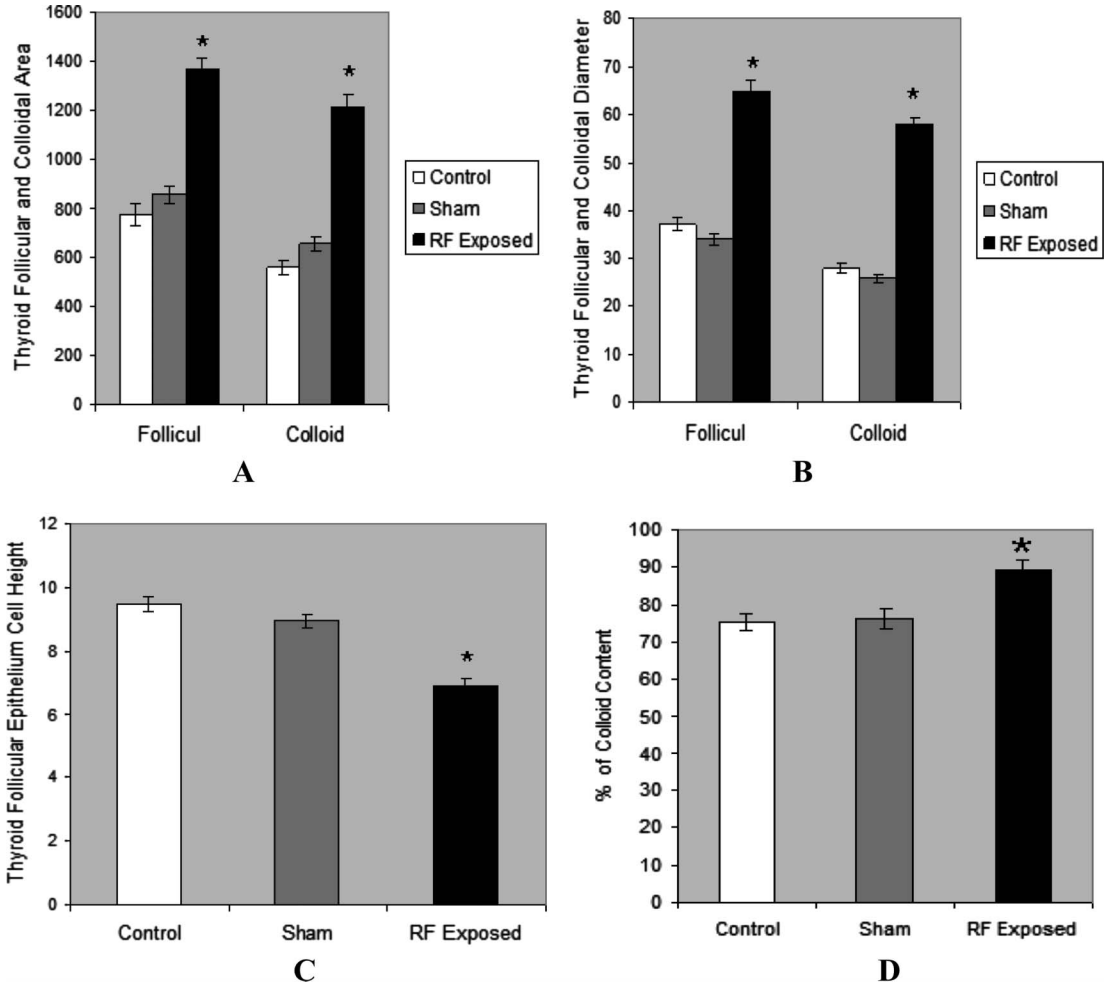

Figure 5. (A) Follicular and colloidal area (μm^2); (B) The follicle and colloid diameter (μm); (C) The height of the thyroid follicular cells (μm); (D) Colloid content. Bars indicate mean $\pm$ SD of 10 independent experiments. *significantly different at $p < 0.001$ by ANOVA.

Moreover the increase in the follicular area and diameter in the RF-exposed group may be associated with the increase in colloidal area and colloidal diameter. Because it is known that the size of a follicle depends on the amount of colloid (Hartoft et al. 2005). These morphometrical results of this study suggest that TH secretion is inhibited by pulse modulated RF radiation.

In addition to the observations of structural changes in the thyroid glands of the RF-exposed group, we also observed increased caspase-3 and caspase-9 activations in thyroid cells of the exposed rats. The distinct formation of typical morphology characteristic indicators – apoptotic bodies in the exposed group with explicit crista lost in mitochondria – indicated that thyroid follicular cells were in apoptotic stage. Our results showed that pulse-modulated RFR can induce caspase-3- and caspase-9-dependent apoptotic pathways in thyrocytes of the thyroid gland and supports the hypothesis that RFR may enhance apoptosis. There are studies reporting controversial results on the activation of caspases and apoptotic responses due to continuous-wave or modulated RF radiation exposure in different cell types. Palumbo et al. (2008) reported increased caspase-3 activation in proliferating human lympochytes that were exposed to a 900 MHz RFR. On the contrary, Merola et al. (2006) and Joubert et al. (2006) found no significant effects on caspase-3 activity in human LAN-5 neuroblastoma and SH-SY5Y neuroblastoma cells after RFR exposure. Marinelli et al. (2004) observed activation of both p53-dependent and p53-independent apoptotic pathways in T-lymphoblastoid leukaemia cells exposed to a 900 MHz continuous-wave RFR at 3.5 mW/kg SAR level for 2–48 h. The human colon cancer LoVo cells showed pathological change of apoptosis after exposure to RFR, whereas normal human WI-38 cells showed no detectable apoptotic response (Maeda et al. 2004). Markkanen et al. (2004). showed that 872 MHz or 900 MHz modulated RFR with a pulse deviation of 0.577 ms and pulse repetition of 217 Hz enhanced Ultraviolet (UV)-induced apoptosis in cdc-48 mutated cells

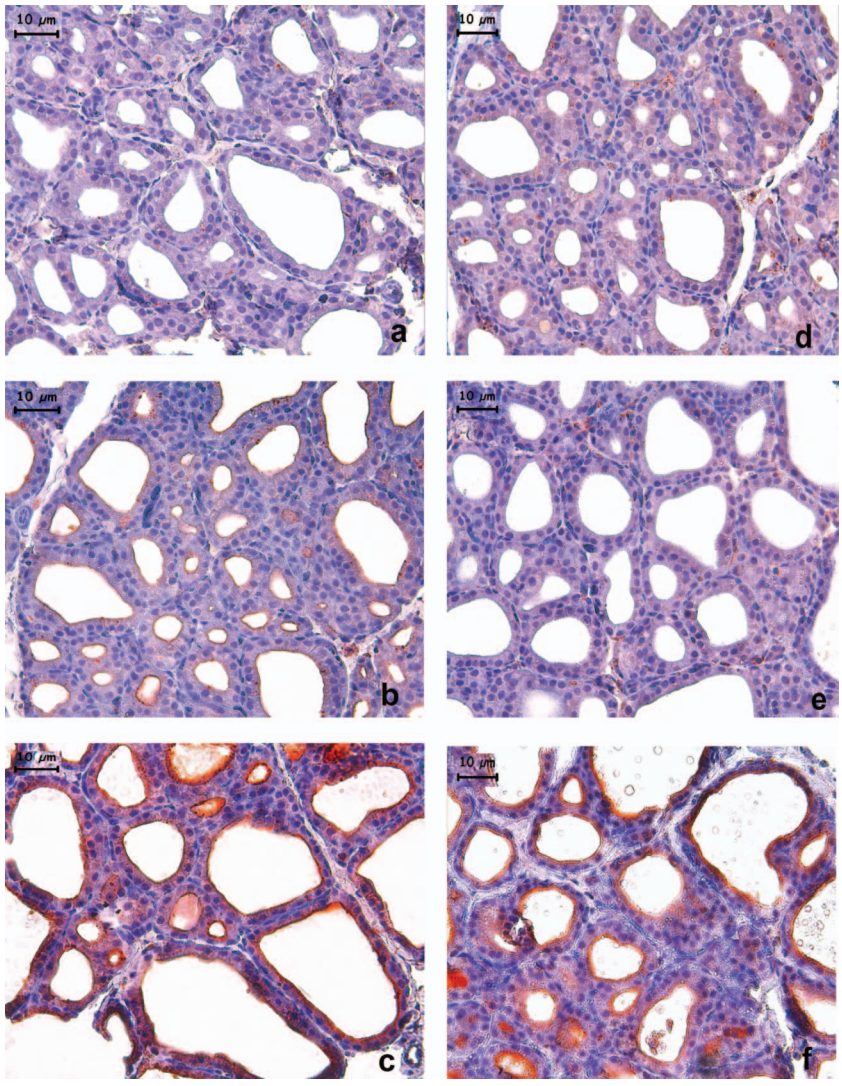

Figure 6. Photomicrographs showing caspase-3 immunoreactivity in representative thyroid samples of control (a), sham (b), and RF-exposed (c) groups. Representative sections of control (d), and sham (e) groups showed occasional slight staining against caspase-9 antibody contrasting with a strong staining pattern in follicular epithelial cells of the RF exposed group (f). Magnifications are at original × 40. Scale bar: 10 μm.

after 1 h of exposure at SAR levels of 0.4 W/kg and 3 W/kg. However, no apoptotic response was observed when the cells were exposed to unmodulated continuous-wave fields at the same SAR levels and time. Lantow et al. (2006) used human Mono Mac 6 cells to investigate whether RFR caused cell cycle, apoptosis or necrosis alterations in cells after exposure to a 1800-MHz RFR at 2 W/kg, The researchers observed no significant change in the cells. Moquet et al. (2008) also did not find any apoptotic response in both proliferating and differentiated murine neuroblastoma (N2a) cells exposed to a 935 MHz RFR at non-thermal level for 24 h. Thus, apoptotic response to RFR may depend on cell type and the conditions of exposure.

Apoptosis may play an important role in thyroid homeostasis and autoimmune diseases including the central pathogenic events in the destruction of thyroid follicular cells in HT which is a disorder that often results in hypothyroidism. Immunohistochemical studies of thyroid tissue sections revealed an increased number of apoptotic follicular cells in HT (Andrikoula and Tsatsoulis 2001). A potentially important pathway in signaling apoptosis in the thyroid involves the Fas death-inducing receptor. Fas is a type I membrane protein and a member of the tumour necrosis factor receptor family. It is found constitutively expressed on lymphocytes and has been detected on many cells of nonhematopoeitic origin. Activation of Fas by Fas-ligand initiates intracellular signals that results in death of the cell. Regulation or modulation of this pathway can occur at multiple levels throughout the pathway (Bretz et al. 1999). Slightly enhanced cell sensitivity to Fas-induced apoptosis was observed in human Jurkat T-cells exposed to a 2.45 GHz continuous-wave

RFR at 4 W/kg for 48 h. The results of the study suggested that RFR acts either on membrane Fas receptor or sphyngomyelinase activation or on Fas pathway between receptor and caspase-3 activation (Peinnequin et al. 2000).

Reactive oxygen species (ROS) generation and overload of cellular calcium [Ca2+] ions may be involved in the alteration of the thyroid morphology and the induction of caspase pathways in thyroid cells. It is known that, after exposure to a significant amount of ROS, TPO (thyroid peroxidase) and subsequent TH formation are inhibited in thyroid cells (Sugawara et al. 2002). TPO is an important enzyme located at the apical membrane of the follicular epithelial cell and catalyses the oxidation of iodine and the synthesis of TH. On the other hand, several lines of evidence support the involvement of ROS in many models of apoptotic cell death (McConkey and Orrenius 1996). Friedman et al. (2007) showed that RFR stimulates plasma membrane NADH oxidase in mammalian cells and causes production of ROS.

Intracellular calcium homeostasis is important for cell survival. In all eukaryotic cells, the cytosolic concentration of Ca2+ ion ([Ca2+]c) is tightly controlled by interactions among transporters, pumps, channels and binding proteins (Giorgi et al. 2008). Under pathological conditions of [Ca2+]c overload, particularly in association with oxidative stress, may trigger pathological states that lead to apoptotic cell death (Duchen 2000). Some studies have reported that RFR may affect electrical properties and ions distributions around the cell by altering calcium pumps within or surface of the cells. Modulated RFR causes calcium ion efflux from cells which could significantly alter the intracellular calcium concentrations (Dutta et al. 1984).

Results of this study indicated that whole body exposure to modulated RFR similar to that emitted by GSM mobile phones caused pathological changes in the thyroid gland by altering gland morphology and inducing apoptotic pathways. Morphological analysis of the thyroid gland demonstrated a high prevalence of cell hypothyrophy altered by the modulated RFR. Immunohistochemical results of this study indicated that the modulated RFR activated caspase-9 and caspase-3 enzymes whose proteolytic activities are the key factor in apoptotic execution. Activated forms of them are markers of cells undergoing apoptosis. Our results suggest an association between mobile phone use and development of HT.

Acknowledgements

This work was supported by the Research Funds of Gazi University (Project nos: 31/2002–07 and 01/2003–62). The authors thank Dr Bahriye Sırav and Dr Seren Giray for their technical assistance.

Declaration of interest: The authors report no conflicts of interest. The authors alone are responsible for the content and writing of the paper.

References

Andrikoula M, Tsatsoulis A. 2001. The role of Fas-mediated apoptosis in thyroid disease. European Journal of Endocrinology 144:561–568.

Apollonio F, D'Inzeo G, Tarricone L. 1997. Theoretical analysis of voltage-gated membrane channels under GSM and DECT exposure. Microwave Symposium Digest Denver: Institute of Electrical and Electronics Engineers Microwave Theory and Techniques Society International. pp 103–106.

Black DR, Heynick LN. 2003. Radiofrequency (RF) effects on blood cells, cardiac, endocrine, and immunological functions. Bioelectromagnetics 6:187–195.

Bretz JD, Arscott PL, Myc A, Baker JR. 1999. Inflammatory cytokine regulation of Fas-mediated apoptosis in thyroid follicular cells. Journal of Biological Chemistry 274:25433–25438.

Buttiglione M, Roca L, Montemurno E, Vitiello F, Capozzi V, Cibelli G. 2007. Radiofrequency radiation (900 MHz) induces Egr-1 gene expression and affects cell-cycle control in human neuroblastoma cells. Journal of Cellular Physiology 213:759–767.

Caraglia M, Marra M, Mancinelli F, D'Ambrosio G, Massa R, Giordano A, Budillon A, Abbruzzese A, Bismuto E. 2005. Electromagnetic fields at mobile phone frequency induce apoptosis and inactivation of the multi-chaperone complex in human epidermoid cancer cells. Journal of Cellular Physiology 204:539–548.

Castillo VA, Rodriguez MS, Lalia JC, Pisarev MA. 2003. Morphologic changes in the thyroid glands of puppies fed a high-iodine commercial diet. International Journal of Applied Research in Veterinary Medicine 1:61–80.

Denef J, Ovaert C, Many MC. 1989. Experimental goitrogenesis. Annals d'Endocrinologie 50:1–15.

De Seze R, Fabbro-Peray P, Miro L. 1998. GSM radiocellular telephones do not disturb the secretion of antepituitary hormones in humans. Bioelectromagnetics 19:271–278.

Duchen MR. 2000. Mitochondria and calcium: From cell signalling to cell death. Journal of Physiology 15:57–68.

Dutta SK, Subramoniam A, Ghosh B, Parshad R. 1984. Microwave radiation-induced calcium ion efflux from human neuroblastoma cells in culture. Bioelectromagnetics 5:71–78.

French PW, Donnellan M, McKenzie DR. 1997. Electromagnetic radiation at 835 MHz changes the morphology and inhibits proliferation of a human astrocytoma cell line. Bioelectrochemistry and Bioenergetics 43:13–18.

Friedman J, Kraus S, Hauptman Y, Schiff Y, Seger R. 2007. Mechanism of short-term ERK activation by electromagnetic fields at mobile phone frequencies. Biochemical Journal 405:559–568.

Garaj V, Gajski G, Trosić I, Pavicić I. 2009. Evaluation of basal DNA damage and oxidative stress in Wistar rat leukocytes after exposure to microwave radiation. Toxicology 259(3):107–112.

Gerald M. 1997. Caspases: The executioners of apoptosis. Biochemical Journal 326:1–16.

Giorgi C, Romagnoli A, Pinton P, Rizzuto R. 2008. Ca2 signaling, mitochondria and cell death. Current Molecular Medicine 8:119–130.

Hardell L, Carlberg M, Söderqvist F, Hansson Mild K. 2008. Meta-analysis of long-term mobile phone use and the association with brain tumours. International Journal of Oncology 32:1097–1103.

Hartoft ML, Rasmussen AK, Rasmussen UF, Buschard K, Bock T. 2005. Estimation of number of follicles, volume of colloid and inner follicular surface area in the thyroid gland of rats. Journal of Anatomy 207:117–124.

Hashimoto Y. 1996. A brief overview of apoptosis. Human Cell 9:194–196.

Hook GJ, Zhang P, Lagroye I, Li L, Higashikubo R, Moros EG, Straube WL, Pickard WF, Baty JD, Roti Roti JL. 2004. Measurement of DNA damage and apoptosis in Molt-4 cells after in vitro exposure to radiofrequency radiation. Radiation Research 161:193–200.

Höytö A, Luukkonen J, Juutilainen J, Naarala J. 2008. Proliferation, oxidative stress and cell death in cells exposed to 872 MHz radiofrequency radiation and oxidants. Radiation Research 170:235–243.

Institute of Electrical and Electronics Engineers/American National Standards Institute (IEEE/ANSI). 1992. IEEE C95.1-1991: IEEE standard for safety levels with respect to human exposure to radio frequency electromagnetic fields, 3 kHz to 300 GHz. New York: IEEE Inc. pp 1–76.

International Commission on Non-Ionizing Radiation Protection (ICNIRP). 1998. Guidelines for limiting exposure to time-varying electric, magnetic and electromagnetic fields (up to 300 GHz). Health Physics 74:494–522.

Ingbar SH. 1985. The thyroid gland. Textbook of endocrinology. 7th ed, London: WB Saunders.

INTERPHONE Study Group. 2010. Brain tumour risk in relation to mobile telephone use: Results of the INTERPHONE international case-control study. International Journal of Epidemiology 2010:1–20.

Joubert V, Bourthoumieu S, Leveque P, Yardin C. 2008. Apoptosis is induced by radiofrequency fields through the caspase-independent mitochondrial pathway in cortical neurons. Radiation Research 169:38–45.

Joubert V, Leveque P, Cueille M, Bourthoumieu S, Yardin C. 2007. No apoptosis is induced in rat cortical neurons exposed to GSM phone fields. Bioelectromagnetics 28:115–121.

Joubert V, Leveque P, Rametti A, Collin A, Bourthoumieu S, Yardin C. 2006. Microwave exposure of neuronal cells in vitro: Study of apoptosis. International Journal of Radiation Biology 82:267–275.

Koyu A, Cesur G, Ozguner F, Akdogan M, Mollaoglu H, Ozen S. 2005. Effects of 900 MHz electromagnetic field on TSH and thyroid hormones in rats. Toxicology Letters 157:257–262.

Lai H, Singh NP. 1996. Single- and double-strand DNA breaks in rat brain cells after acute exposure to radiofrequency electromagnetic radiation. International Journal of Radiation Biology 69:513–521.

Lantow M, Viergutz T, Weiss DG, Simkó M. 2006. Comparative study of cell cycle kinetics and induction of apoptosis or necrosis after exposure of human mono mac 6 cells to radiofrequency radiation. Radiation Research 166:539–543.

Luukkonen J, Hakulinen P, Mäki-Paakkanen J, Juutilainen J, Naarala J. 2009. Enhancement of chemically induced reactive oxygen species production and DNA damage in human SH-SY5Y neuroblastoma cells by 872 MHz radiofrequency radiation. Mutation Research 662:54–58.

Lin JD. 2001. The role of apoptosis in autoimmune thyroid disorders and thyroid cancer. British Medical Journal 322:1525–1527.

Maeda K, Maeda T, Qi Y. 2004. In vitro and in vivo induction of human LoVo cells into apoptotic process by non-invasive microwave treatment: A potentially novel approach for physical therapy of human colorectal cancer. Oncology Reports 11:771–775.

Marinelli F, La Sala D, Cicciotti G, Cattini L, Trimarchi C, Putti S, Zamparelli A, Giuliani L, Tomassetti G, Cinti C. 2004. Exposure to 900 MHz electromagnetic field induces an unbalance between pro-apoptotic and pro-survival signals in T-lymphoblastoid leukemia CCRF-CEM cells. Journal of Cellular Physiology 198:324–332.

Markkanen A, Penttinen P, Naarala J, Pelkonen J, Sihvonen AP, Juutilainen J. 2004. Apoptosis induced by ultraviolet radiation is enhanced by amplitude modulated radiofrequency radiation in mutant yeast cells. Bioelectromagnetics 25:127–133.

McConkey DJ, Orrenius S. 1996. Signal transduction pathways in apoptosis. Stem Cells 14:619–631.

Merola P, Marino C, Lovisolo GA, Pinto R, Laconi C, Negroni A. 2006. Proliferation and apoptosis in a neuroblastoma cell line exposed to 900 MHz modulated radiofrequency field. Bioelectromagnetics 27:164–171.

Moquet J, Ainsbury E, Bouffler S, Lloyd D. 2008. Exposure to low level GSM 935 MHZ radiofrequency fields does not induce apoptosis in proliferating or differentiated murine neuroblastoma cells. Radiation Protection Dosimetry 131:287–296.

Pacini S, Ruggiero M, Sardi I, Aterini S, Gulisano F, Gulisano M. 2002. Exposure to global system for mobile communication (GSM) cellular phone radiofrequency alters gene expression, proliferation, and morphology of human skin fibroblasts. Oncology Research 13:19–24.

Palumbo R, Brescia F, Capasso D, Sannino A, Sarti M, Capri M, Grassilli E, Scarfì MR. 2008. Exposure to 900 MHz radiofrequency radiation induces caspase-3 activation in proliferating human lymphocytes. Radiation Research 170:327–334.

Peinnequin A, Piriou A, Mathieu J, Dabouis V, Sebbah C, Malabiau R, Debouzy JC. 2000. Nonthermal effects of continuous 2.45 GHz microwaves on Fas-induced apoptosis in human Jurkat T-cell line. Bioelectrochemistry 51:157–161.

Sugawara M, Sugawara Y, Wen K, Giulivi C. 2002. Generation of oxygen free radicals in thyroid cells and inhibition of thyroid peroxidase. Experimental Biology and Medicine 227:141–146.

Wollman SH, Herverg JD, Tachiwaki D. 1990. Histologic changes in tissue components of the hyperplastic thyroid gland during its involution in the rat. American Journal of Anatomy 198:35–44.

Zhou XR, Yuan HP, Qu W, Ma CY, Li HY, Wang Y. 2008. The study of retinal ganglion cell apoptosis induced by different intensities of microwave irradiation. Ophthalmologica 222:6–10.

Zmyślony M, Politanski P, Rajkowska E, Szymczak W, Jajte J. 2004. Acute exposure to 930 MHz CW electromagnetic radiation in vitro affects reactive oxygen species level in rat lymphocytes treated by iron ions. Bioelectromagnetics 25:324–328.